The Growth Characteristics of Small Cumulus Clouds

MORTON GLASS

Air Force Cambridge Research Laboratories

AND TOBY N. CARLSON[1]

Weather Services, Inc.

(Manuscript received 15 October 1962, in revised form 25 April 1963)

ABSTRACT

The vertical growth, diameters and trajectories of cumulus clouds observed over the San Francisco Peaks near Flagstaff, Ariz., were determined from photogrammetric measurements. New clouds formed in a small, well defined area. Their trajectories indicate the complex nature of orographic effects on the wind field. Active cloud elements were found to have growth characteristics similar to thermals observed in laboratory experiments. In particular, thermals broadened with height along a cone whose interior angle was about 30°, increasing their volumes by an order of magnitude prior to destructive erosion. Computed values of buoyancy decreased from a maximum initially, approaching zero or becoming negative near the erosion level, depending on the form of the momentum equation used.

1. Introduction

The development and verification of cumulus convection theories have been restricted, in part, by difficulties in obtaining accurate measurements of relevant parameters. With the use of precise photogrammetric techniques, it is possible to measure height and diameter changes accompanying the growth and decay of individual cloud elements in small cumuli. The purpose of this paper is to apply these techniques to such an investigation and to interpret the reduced data in terms of present convection models. This study is concerned primarily with a group of cumulus clouds which formed in the vicinity of the mountain peaks near Flagstaff, Ariz., on 19 July 1960. In addition, some features of the environment are deduced from cloud trajectories.

2. Observational techniques

a. *Camera locations and orientation.* The data presented in this paper were collected during the Air Force Cambridge Research Laboratories' Project "High Cue" program which was conducted in the region of the San Francisco Peaks near Flagstaff, Ariz. The measurements were obtained by means of a pair of ground-based Air Force T-11 mapping cameras. Simultaneous photographs were taken every minute to obtain a time lapse history of cloud growth in stereoscopic view. The cameras were located at the ends of a baseline oriented perpendicular to the azimuth W4.6°N, and were mounted so that the focal plane was perpendicular to the horizontal. Measurements were made with respect to the State Plane Coordinate system. Use of these coordinates simplifies the referencing of cloud positions and movement with respect to topography and wind direction, and provides a means for easy comparison with other data. In addition, these coordinates offer a simple way of maintaining continuity in a series of measurements if a shift in camera orientation is made. The Y coordinate (grid north) is closely comparable with geographic north in the Flagstaff area (grid north = E0.15°N). Relative positions of the camera sites derived from measurements on Mt. Elden, a main triangulation station, were placed in the State Plane Coordinate system by referring the measured angles to a second triangulation station. Distance was determined with a tellurometer, angular values with a Wilde T-2 theodolite. Internal checks proved the consistency of the triangulation. All measurements were repeated in order to reduce random error. Camera locations and baseline were chosen so that the requirements of good stereo vision and maximum parallax differences were compromised to effect a high degree of accuracy in spite of the great variations in depth to be encountered in cloud measurements over the area. The derived camera baseline was 8860±6 ft. Fig. 1 shows the location of the camera sites and their normal field of view with respect to the San Francisco Peaks area.

b. *Measurement precision.* The photogrammetric analysis procedure is based on the principle of parallax measurement to determine the range Y of a point in space. Since the cameras' optical axes were approximately parallel and oriented horizontally, the analysis procedure can be represented by the equations for the

[1] Now at Imperial College, London.

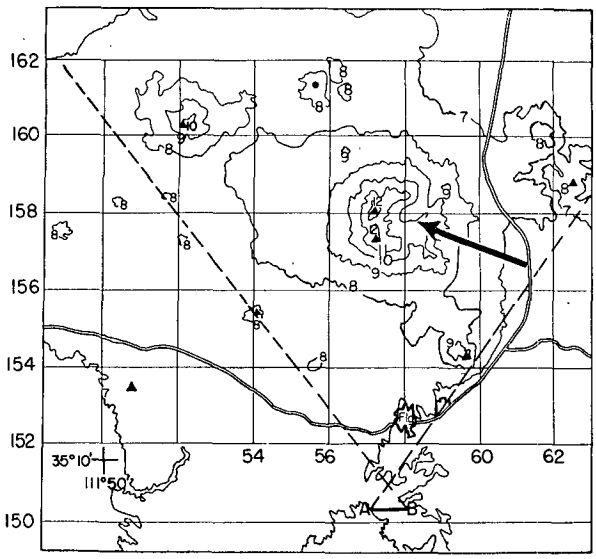

FIG. 1. Map of San Francisco Peaks area. Grid labeled in tens of thousands of feet from state plane origin. Ground elevation contours labeled in thousands of feet. Arrow represents azimuth of sun at 1030 MST, 19 July. Dotted line shows field of view of stereo cameras A and B.

normal case of photogrammetry,

$$Y=\frac{B_x}{p}F, \tag{1}$$

where B_x is the baseline distance perpendicular to the camera axis and F is the focal length. In Fig. 2, parallax p, $(x'-x'')$, is the difference from the same cloud protuberance to a reference on each of the photographs. Once the range and thus the scale B_x/p is known, the coordinates

$$X=\frac{B_x}{p}x' \tag{2}$$

and

$$Z=\frac{B_x}{p}z' \tag{3}$$

can be determined. The coordinates X and Z are positive eastward and upward, respectively. The values x' and z' are adjusted coordinate measurements made with respect to fiducial lines on the reference photograph. Adjustment for deviations of the camera pair from the normal case and the final output in State Plane coordinates required several matrix rotations of intermediate coordinate systems and have been programmed for an IBM 650 computer by D. R. Schurz and J. G. Houle of the Department of Civil and Sanitary Engineering at Massachussetts Institute of Technology.

It was desired that the analysis procedure satisfy two criteria: the correct location of the cloud in the coordinate system, and the precise measurement of horizontal and vertical velocities. The ability to specify cloud location depends primarily on determination of camera orientation errors. Such errors are systematic and were about 0.5 per cent for clouds fifteen miles from the cameras. Vertical growth ΔZ, and horizontal movement ΔX, ΔY of cloud protuberances were derived from micrometer measurements obtained on a Zeiss Stereotope. Studies made of factors contributing to random errors indicate higher precision has been attained than heretofore reported (Orville and Kassander, 1961). Measurements made in computing range parallax contained the major source of error. Fig. 3 shows the extent

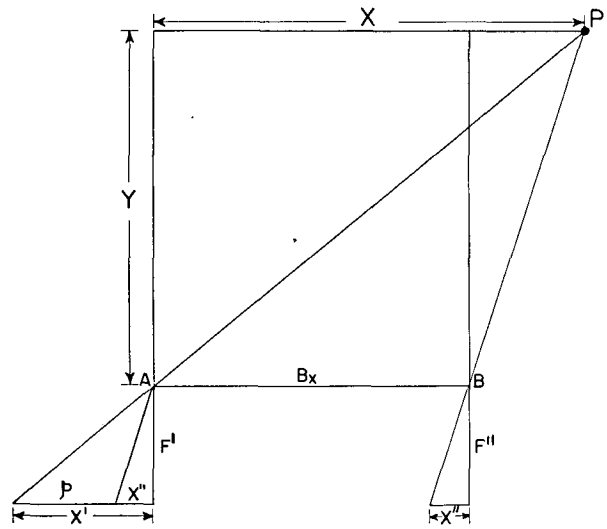

FIG. 2. Geometry for parallax; measurement—normal case. Position $P(X,Y)$ is determined from parallax p, $(x'-x'')$, baseline B_x, and focal lengths F' and F'' measured on photographs from cameras A and B, respectively.

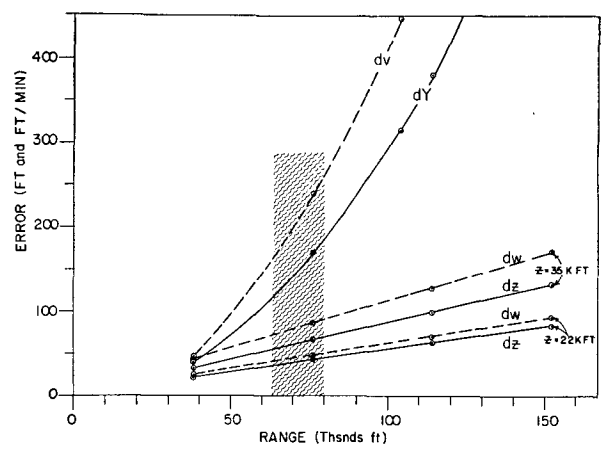

FIG. 3. Standard error of measurement precision due to random causes versus range. Curves labeled dY and dv represent precision in measuring range and velocity along Y component. Errors in measuring height dZ and vertical velocity dW are shown for two representative heights (above sea level). Hatching shows range pertinent to this study. Errors in X are similar to those in Z.

of random position error dY, dZ, and the velocity error dv and dW. Data presented in this figure are based on conservative estimates. Errors in X were omitted since they are similar to those in Z. It should be noted that dW is small compared to the magnitude of the vertical velocities.

c. *Definitions.* Careful examination, with a stereo viewer, of a series of small clouds that formed near Humphreys Peak revealed that many consisted of one or a few easily definable elements. These elements could be examined separately, and in many cases followed through the course of their development. This suggested a method of approach to the data based on the bubble concept as originally described by Scorer and Ludlam (1953).

For the purpose of objectivity, the following definitions are employed: A cloud thermal (hereafter referred to as a thermal) is a cloud element which develops as a separate entity distinct from its surroundings with respect to buoyancy and momentum. Observations of thermals indicated that the upper surface (or cap) was often rounded. Below the cap, the thermal's shape resembled a circular cylinder. Diameters were measured near the top of the cylindrical section and their positions relative to the cap maintained as long as possible. The word "bubble" refers to a hypothetical sphere whose upper surface forms the hemispherical cap. A cloud is defined as an agglomeration of thermals and thermal residues. All small clouds studied here were composed of three or fewer thermals. In cumulus containing more than one thermal, cloud bases appeared as an aggregate of individual thermal bases.

Since the thermals existed for a relatively short time (usually five to ten minutes), the motions of the cap were adequately represented by three dimensional position changes with time of a few well defined protuberances (tufts) on the cloud. Anderson (1960) has shown that the vertical velocity of the tuft represents the thermal's vertical motion, provided the tuft remains close to the vertical axis of the thermal. Tufts which mix with the environmental air are displaced to the sides, eventually losing their identity and evaporating. New material emerging from the interior replaces the old. Observations here confirmed this sequence of events.

It was possible to delineate twenty-one thermals that could be followed through all or most of their existence. The observation period on the day studied began at 1010 MST, just after the onset of convective cloud

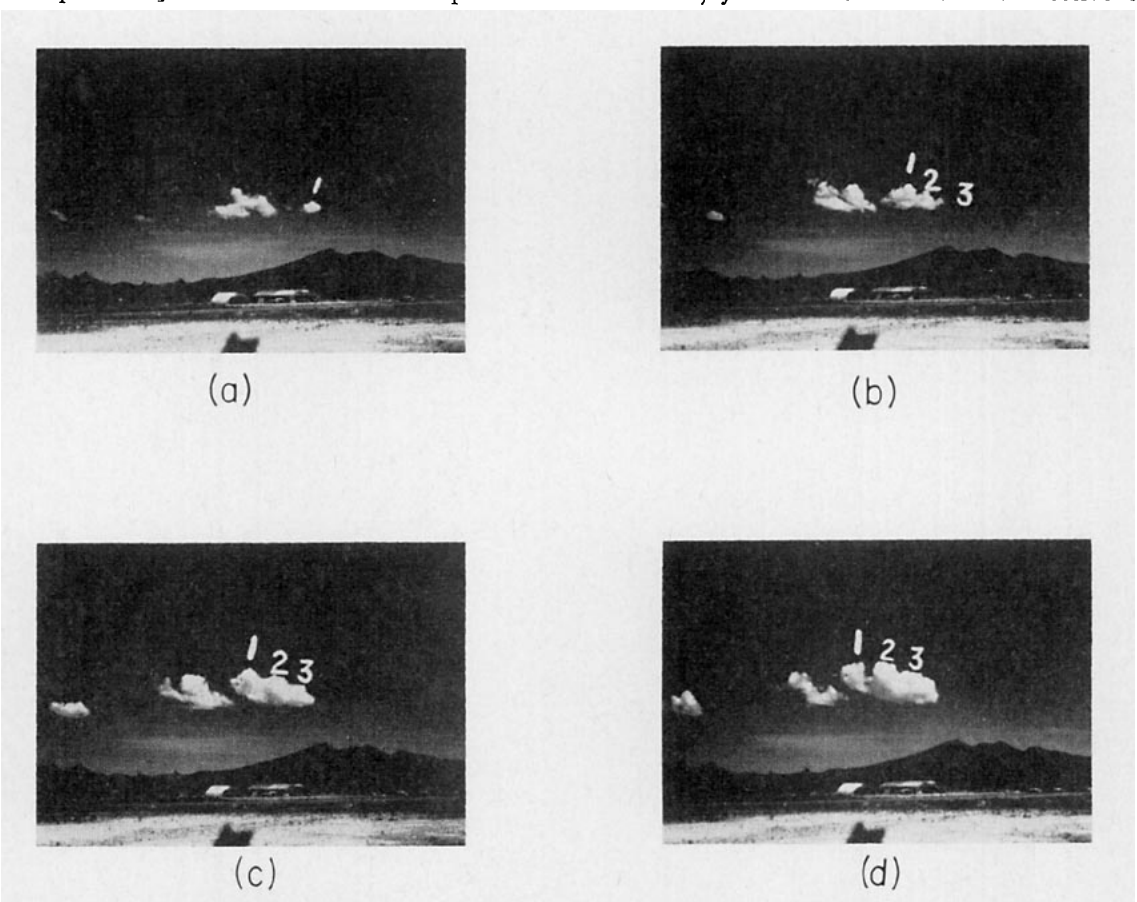

FIG. 4. Growth sequence: Cloud 4—Thermals 1, 2, 3, Interval between photographs is three minutes. Note marked erosion of thermal 1 in (d).

activity, and ended at 1120 when all clouds in the vicinity of the peak began to decay. Photographs of cloud 4, from which three thermals were distinguished, are presented in Fig. 4. The time sequence of tuft heights was fitted to a smoothed curve representing the thermal's height (Fig. 5). A single tuft was often sufficient to provide complete information concerning both height and vertical velocity of the thermal cap.

3. Results

a. *Relation between clouds and terrain.* Braham and Draginis (1960) and Silverman (1960) have made detailed studies on the effect of a mountain ridge on convection. They found isolated regions or "cores" of excess temperature and humidity below cloud level. They reasoned that forced lifting of air, caused by the barrier, was obscured by the more important effect of surface heating. As the valley breeze moves up the mountain slopes, adiabatic cooling is offset by nonadiabatic warming due to solar heating. The latter furnishes the energy needed to initiate a thermally driven circulation. Upon reaching the mountain summit, the heated air continues to rise due to its excess virtual temperature. Particularly favored portions of the rising air attain saturation and appear as cumulus clouds. It is likely that the heating process in the San Francisco Peaks is more important than mechanical lifting.

The interactions of these two processes, lifting and heating, are enormously complicating factors in determining the wind field and cloud source regions over mountainous terrain. The studies cited above indicate that orographic lifting alone is not sufficient to initiate cumulus cloud formation during summer conditions in the Southwest. The San Francisco Peaks, the region of this present study, represent an isolated projection extending several thousand feet above the plateau. This is conducive to an airflow around the barrier, rather than over it.

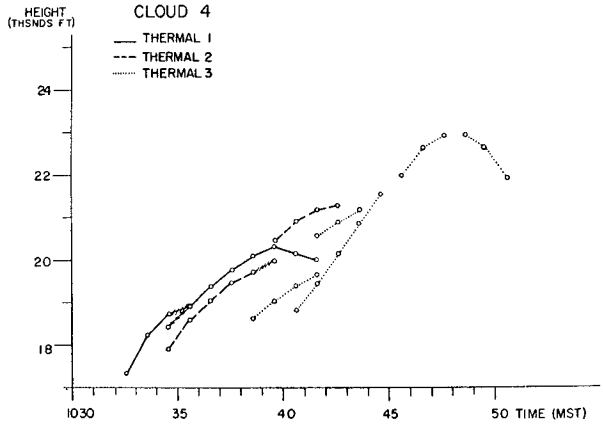

FIG. 5. Tuft height versus time for three thermals comprising cloud 4. Hatch marks show portion of trace not representative of thermal cap. Thermal heights given by tuft height or average of overlapping tufts.

During the morning of 19 July, the sun's azimuth was east-southeast with respect to the peaks (Fig. 1). Therefore, the greatest heating was on that side. An examination of the photographs indicated that cumuli formed in a small area immediately downstream from the peak. In view of the thermal trajectories (Fig. 6) and the radiosonde winds (Fig. 11) it seems likely that the subcloud origin of the thermals was northeast of Humphreys Peak. This supports a belief that upslope wind, however small, is important in determining the location of initial cloud formation. Cloud elements appeared to rise vertically, then accelerate downstream, becoming more tilted as they progressed. The fact that thermals became tilted with time indicated that their updraft was weakening because of mixing.

The assumption was made that dissipating thermals had thoroughly mixed their momentum with that of the surrounding air. Therefore, the u, v components, determined from the X, Y position changes of tufts whose vertical velocity had decreased to a negligible value, were assumed to represent the ambient wind. Horizontal tuft velocities were tabulated, and the data stratified into three vertical layers according to tuft height: 17,500 to 20,000, 20,000 to 22,500 and 22,500 to 25,000 ft. Fig. 7 is an analysis of the wind field at the lowest layer. It must be emphasized that the analyses are presented as a schematic reflection of actual wind conditions. The paucity of data precludes any detailed interpretation. Some additional data points outside the area presented in Fig. 7 were used in the analysis. The vertical cross section (Fig. 8) shows a reasonable consistency between wind patterns deduced at each level.

Figs. 7 and 8 illustrate marked small scale spatial

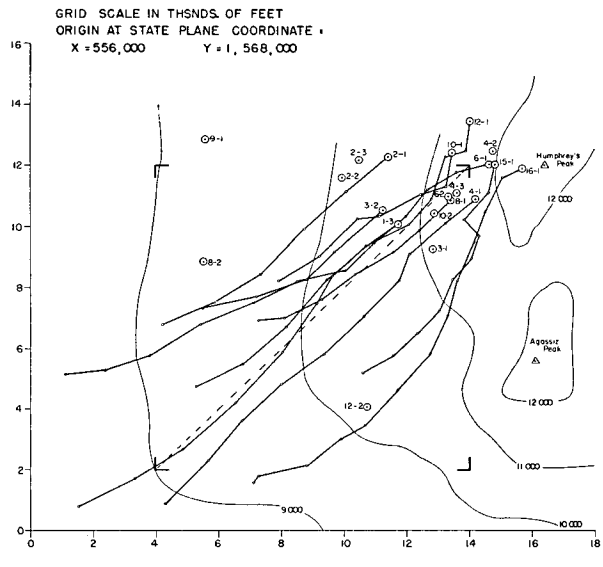

FIG. 6. Trajectories of ten cumulus thermals (dark, solid lines) and initial positions of these and ten others labeled by cloud and thermal number (large circles). Light, solid lines represent ground elevation contours (ft.). Boundaries of Fig. 7 outlined by dark corners.

fluctuations in the wind flow. One explanation for undulations in the velocity is that convection, causing a vertical exchange of horizontal momentum, induced significant variation in the cloud level wind field by enhancing the effect of the mountain. This would account for lighter winds being observed near the peaks, and suggests that the wind field over heated mountainous terrain is too complex for cumulus entrainment rates to be studied on a simple momentum exchange basis as done by Malkus (1952).

b. *Small cumulus.* Thermal diameter and vertical velocity were plotted versus height of the thermal cap for twenty-one cases which failed to grow to congestus. Thermals associated with small cumulus clouds exhibited one complete growth cycle and dissipated without benefit of additional pulsations as is characteristic of the congestus stage. Six examples are presented in Fig. 9. Data points have been plotted at one minute intervals, the vertical velocity having been computed from the centered differences of successive height values. Smoothed curves were drawn through the sequence of heights and velocites. Single points, which were thought to reflect a gross measurement error, were not included in the analyses.

Almost all twenty-one thermals exhibited a progressive diameter increase with height up to some level. There, a dramatic change occurred in the growth of the convective element. The thermal continued to rise, but at a much slower rate than before, and the diameter ceased broadening and actually began to decrease. Finally, there was a complete disintegration of the thermal. Although there was a general trend for the vertical velocity to decrease with height, the greatest decelerations occurred immediately at the level where the thermal began to erode. This level will be referred to as the erosion height, Z_e.

There is a special significance in the fact that the thermals broadened with height along a cone. If D and Z represent the diameter and height of the thermal cap and the subscript e refers to the erosion level, then

$$D=m(Z-Z_0) \quad Z<Z_e, \tag{4}$$

where m is the broadening coefficient of the thermal, and Z_0 the thermal virtual origin.

Essential features of the data are presented in Table 1 where Z_{max} refers to the maximum thermal height, W represents vertical velocity of the cap, and the subscript b applies to quantities determined at the cloud base level.[2] Occasionally, the thermal's active life span was so short that fewer than two measurements were available below Z_e. In such cases, no value of m was computed; e.g., cloud 3, thermal 1. Most broadening ratios were between 0.50 and 0.58, although a few exceeded 0.80. From thermals that newly emerged from cumulus congestus, Saunders (1961) inferred for the saturated interior of the cloud a broadening coefficient with a close

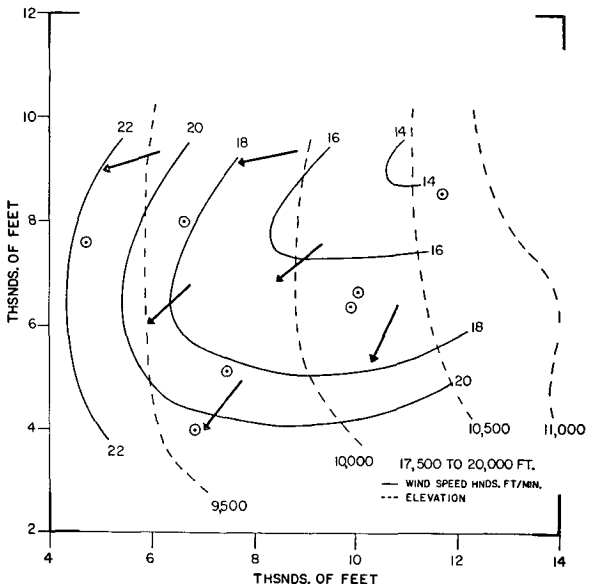

FIG. 7. Analysis of wind regime deduced from trajectories of tufts for the levels 17,500–20,000 ft. Arrows are schematic of wind direction. Area outlined by dark corners similarly outlined in Fig. 6. Dots are data points which fall within outlined area.

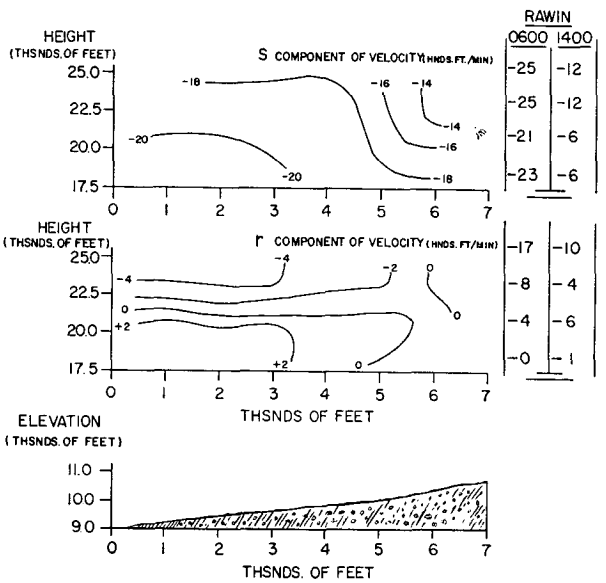

FIG. 8. Vertical cross section of deduced s and r wind components, with the origin identical to that in Fig. 7. The horizontal velocity s is positive along dashed line (Fig. 6) from lower left to upper right. The velocity r is its orthogonal coordinate in the horizontal plane and is positive toward lower right. Wind components obtained from local soundings shown at right for comparison.

[2] It should be pointed out that broadening may be observed independently of an incorporation of new air into the thermal. This will occur in a spherical thermal until the depth $Z-Z_b$ reaches $D/2$, due only to an increasing fraction of the original dry thermal passing the condensation level. In general, this limit was exceeded very early in the thermal's growth, and therefore the computed broadening was considered a true volume increase (see Fig. 9, cloud 6, thermal 1).

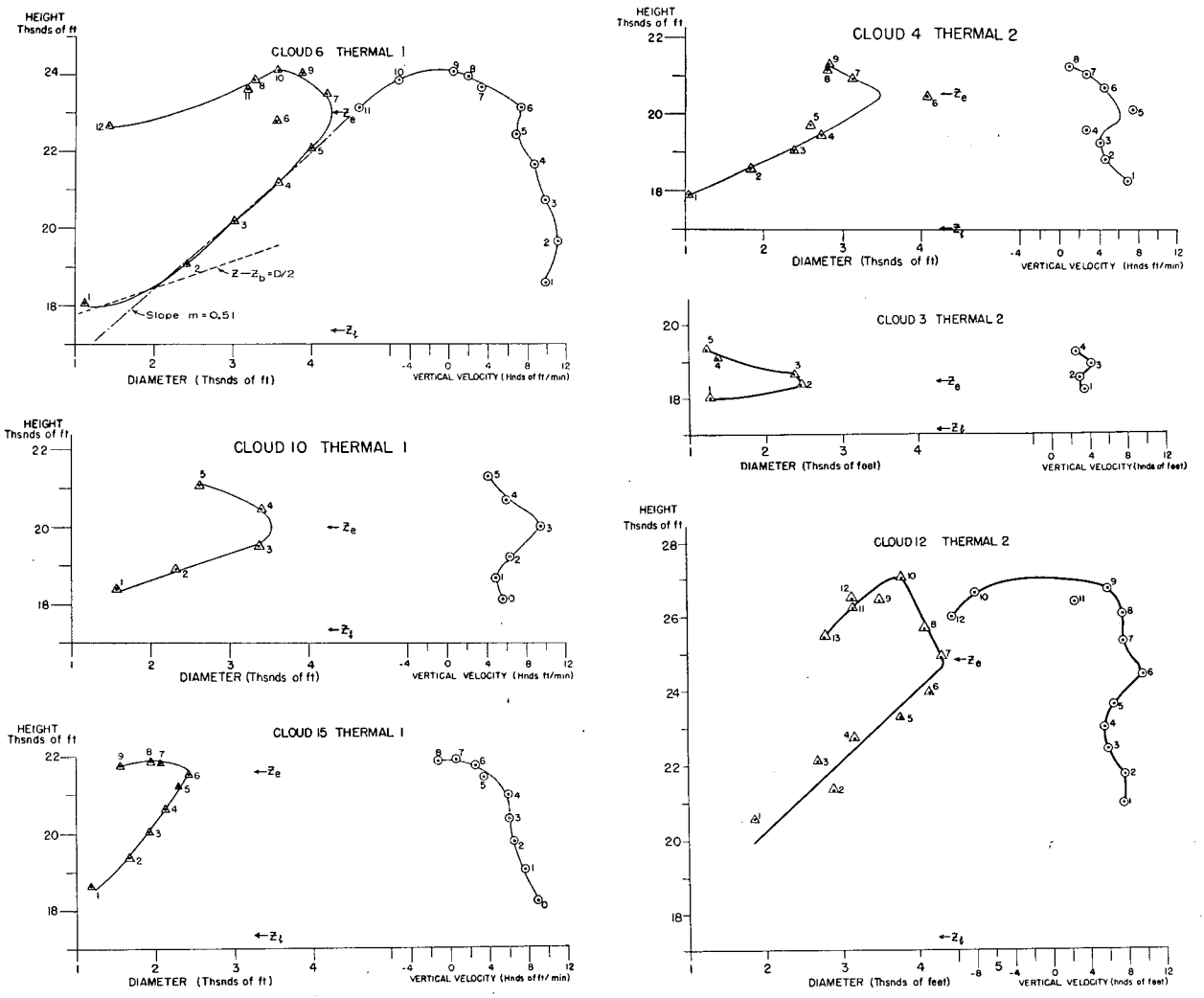

FIG. 9. Height of thermal versus diameter and vertical velocity. Cloud base (Z_b) and erosion level (Z_e) indicated. Data points are numbered sequentially.

scatter of values about 0.40 for a range of widely differing atmospheric conditions.

Values of D_b and Z_0 computed from equation 4 were more variable than the measured broadening coefficient, m. Generally, taller thermals had lower virtual origins and larger diameters at formation, a result which supports the concept of "protected cores" as described by Malkus (1960). In fact, the correlation between the depth, $Z_{max}-Z_b$, and D_b was 0.74. In clouds with depths exceeding 2000 feet, the maximum depth appears to have little dependence on the initial vertical velocity W_b. (The earliest measurement of vertical velocity was considered the best estimate for W_b).

The clouds grew through two relatively dry, stable layers, one between 18,500 and 20,000 ft, and the other between 22,500 and 25,000 ft. (See lapse rate, Fig. 11). Fig. 10 shows a scatter of points for both Z_e and Z_{max} versus the time at which erosion occurred. The curves in this figure illustrate the inhibiting effect on the cumulus by slight decreases in the lapse rate. The fact that values of Z_e tended to cluster about the base of the more stable layers suggests that erosion is associated with a depletion of the thermal's buoyancy. The amount of "over-shoot" $Z_{max}-Z_e$ varied between 0.1 and 0.7 of the diameter at erosion, but this quantity was not obviously dependent on any one factor.

Observations from photographs revealed that noticeable changes occurred in the structure of the thermal at erosion. During the stage of active growth when broadening was essentially linear, bases were flat and well defined, while the upper surfaces of the element retained a hard appearance. After erosion, bases became ragged and the upper surfaces appeared fuzzy and indistinct. It is obvious then, that the observed broaden-

TABLE 1. Cumulus humilis. Summary of data on thermals. Columns labeled: Cloud and thermal; maximum height of thermals, $Z_{max}-Z_b$; erosion height, $Z_{max}-Z_e$; diameter at erosion, D_e; vertical velocity at erosion, W_e; estimated vertical velocity at cloud base level, W_b; calculated virtual origin, Z_0; calculated diameter at cloud base level, D_b; and broadening coefficient, m. Quantities which were unobtainable are indicated by dots. The cloud base Z_b was 17,300 ft. Starred thermals are illustrated in Fig. 9.

Cloud and thermal	$Z_{max}-Z_b$ (ft)	$Z_{max}-Z_e$ (ft)	D_e (ft)	W_e (ft min^{-1})	W_b (ft min^{-1})	Z_0 (ft)	D_b (ft)	m
2–1	1,200	250	1000	200	500	...	...	...
1–3	1,500	550	3200	230	100	...	...	...
3–1	1,500	600	1100	300	300	...	...	...
2–3	1,950	1000	1500	200	200	...	...	...
2–2	2,000	600	1800	390	460	...	...	...
3–2*	2,000	900	2500	300	350	...	...	...
4–1	3,000	900	2800	440	500	15,900	1260	0.87
9–1	3,500	1500	2600	420	...	...	...	...
10–1*	3,950	750	3500	500	700	16,900	160	1.05
4–2*	4,200	1500	3500	950	570	17,330	30	1.50
15–1*	4,600	300	2400	350	900	15,200	850	0.38
16–1	5,500	1100	3100	550	580	15,400	1010	0.52
4–3	5,600	200	6000	420	480	15,500	1320	0.85
6–2	5,600	700	4500	390	...	13,950	1870	0.55
12–1	5,900	700	4600	500	520	13,200	2020	0.50
8–2	6,300	600	2600	660	...	...	...	...
6–1*	6,900	1200	4250	550	990	14,220	1600	0.51
5–1	6,900	1950	6200	790	720	11,600	3130	0.58
10–2	7,500	100	4500	220	...	15,850	820	0.50
12–2*	9,450	2000	4370	860	...	16,300	750	0.55
8–1	≫3,800	...	>5750	...	480	9,650	3620	0.50

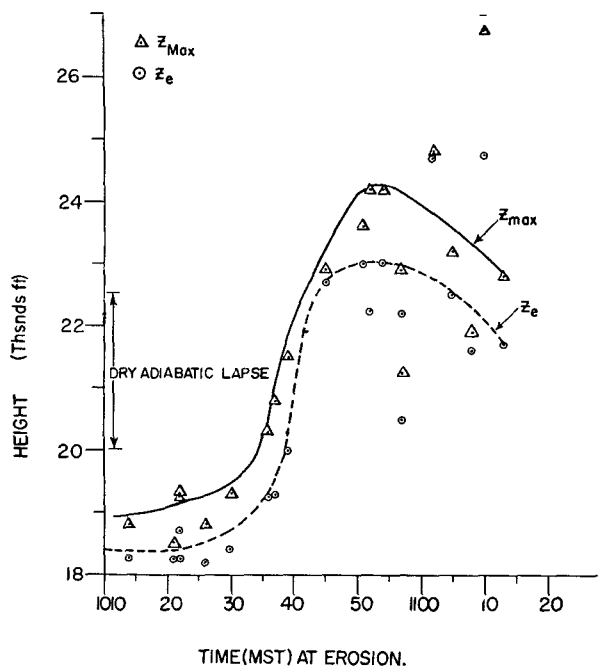

FIG. 10. Maximum and erosion heights versus the time at which erosion occurred for twenty thermals.

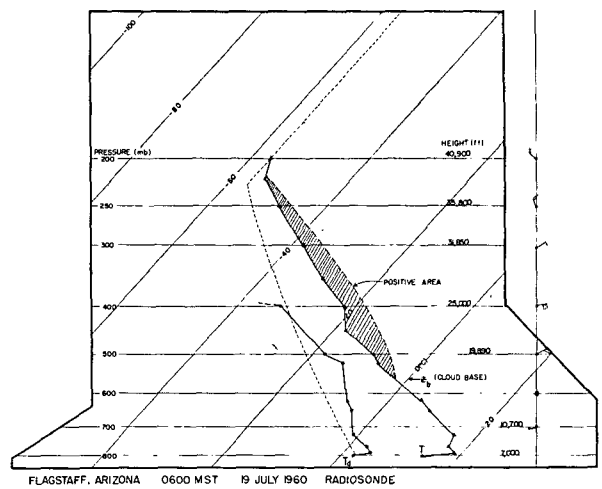

FIG. 11. Skew-T diagram for Flagstaff, Arizona, 0600 MST, 19 July 1960. Shading represents positive area obtained by lifting a parcel moist-adiabatically from the cloud base.

ing is a measure of entrained ambient air. Flights through growing cumuli (Plank, 1959) have revealed a narrow transition zone of temperature and water vapor along the edges, and a relatively uniform medium throughout the interior. Such clouds were generally buoyant; whereas, the ragged ones were relatively cold.

4. Comparison with model experiments

The "bubble" theory of Scorer and Ludlam (1953) introduced the idea of the buoyant parcel (or bubble) as the smallest element in atmospheric convection. Later, Scorer (1957), Hall (1960) and Woodward (1959), on the basis of tank experiments with mud and oil slurries postulated bubble models which included entrainment and detrainment occurring with an internal vortex-like circulation. It was found in these experiments that ideal thermals, advancing through neutral surroundings, expanded along a cone whose interior angle

prescribed a broadening coefficient of about 0.5. Levine (1959), Mason and Emig (1961), and Saunders (1962) extended these ideas, applying them to more complicated bubble models. Recently, Turner (1962) demonstrated that buoyant plumes in a tank exhibited both the features of a non-steady thermal and a steady jet. In his study the buoyant plume was a source of a portion of the material entrained into the leading cap. In addition, numerical studies of Ogura (1962) and Lilly (1962) have supported the concept of buoyant thermals which expand as they rise. A summary of the above studies with respect to broadening is shown in Table 2.

TABLE 2. Summary of broadening coefficients determined in various studies.

Experiments	m	Investigations
Tank (thermal)	0.5	Scorer (1957)
Tank (thermal and plume)	0.3	Turner (1962)
Numerical	0.4	Ogura (1962)
Numerical	0.8	Lilly (1962)
Observational	0.4	Saunders (1961)
Observational	0.5	Present study

Photogrammetric evidence has supported the concept that cumulus clouds develop from a succession of buoyant elements called thermals. Atmospheric thermals can be further compared to those observed in the laboratory. Following Scorer, the relation between the velocity of the thermal cap and the element's buoyancy is

$$W^2=C^2g\bar{B}\frac{D}{2} \tag{5}$$

where $g\bar{B}$ is the mean buoyancy of the thermal. In the atmosphere $\bar{B}=\overline{\Delta\theta}/\theta_0$ where $\overline{\Delta\theta}$ is the mean excess virtual temperature, and θ_0 is the virtual temperature of the environment. The constant C^2 is a Froude number, being the ratio between inertia forces and buoyancy forces. The acceleration of gravity is denoted by g, the vertical velocity of the thermal cap by W, and D has the same meaning as in equation (4).

Saunders has computed an extreme range of C between 0.8 and 2.4 in the atmosphere, as compared with values of 1.2 in the Scorer experiments. In subsequent discussion, C will be assigned the value of 1.2 in order to compute $\overline{\Delta\theta}$. Previously, application of this equation to cumulus cloud measurements was not considered feasible except in a saturated environment. Unfortunately, most thermals emerging from existing clouds soon show signs of destructive erosion due to mixing with a drier environment. In this study, (5) is thought to be applicable up to Z_e because the thermals, followed from their initial formation, broadened in a manner similar to that found in laboratory experiments. Reasonable values of excess virtual temperature computed from (5) would also support the concept of a similarity between tank experiments and atmospheric thermals.

Inherent in the tank models was the conservation of density deficiency or total buoyancy, $g\bar{B}M$ (M = bubble's mass). Introducing this requirement into equations (4) and (5) yields the result that vertical velocity decreases inversely as the distance from the virtual origin; or that

$$(Z-Z_0)^2k=t. \tag{6}$$

where k is a constant and t is time. Some cloud thermals appeared to follow closely this same relation during broadening, (see Figs. 12a), although comparison was unfavorable in over one-third the cases. While a true conservation of total buoyancy probably does not occur in cloud thermals, there is a tendency in this direction since condensation increases buoyancy while evaporation destroys it.

A more general momentum equation, which is also used to describe the growth of buoyant elements, sets the rate of change of forward momentum of the thermal equal to the buoyancy force acting on the thermal; or

$$\frac{d}{dt}(\alpha MW)=g\bar{B}M, \tag{7}$$

where α is a virtual mass coefficient, taken here as 1.5. [The value chosen is comparable to a choice of $C=1.2$ for the case of neutral stability (Saunders, 1962).] Ignoring density changes in the vertical and assuming the thermal's mass is proportional to D^3, equation (7) is expanded to yield:

$$\frac{dW}{dt}+\frac{3W^2}{D}\frac{dD}{dZ}=\frac{1}{\alpha}g\bar{B}. \tag{8}$$

Buoyancy is now expressed as the sum of two measurable components; one expressing vertical acceleration and the other entrainment.

Figs. 12b show a comparison between values of buoyancy, expressed in terms of excess virtual temperature computed from equations (5) and (8). While both curves tend to decrease toward the erosion level, results from the latter equation indicate a sign change in the buoyancy force slightly below Z_e. Neither expression presents an unreasonable description of thermal buoyancy, although the range of values derived from (8) appear somewhat high in view of measurements made by Cunningham, Plank and Campen (1956). Examination of equation (8) in light of Fig. 9 clearly indicates that $\bar{B}$ must change sign very near the erosion level.

5. Summary

The photogrammetric technique described has resulted in precise measurements of cloud dimensions and motion. The technique can also be applied to define a representative wind field in the vicinity of clouds. Careful examination of stereoscopic photographs revealed

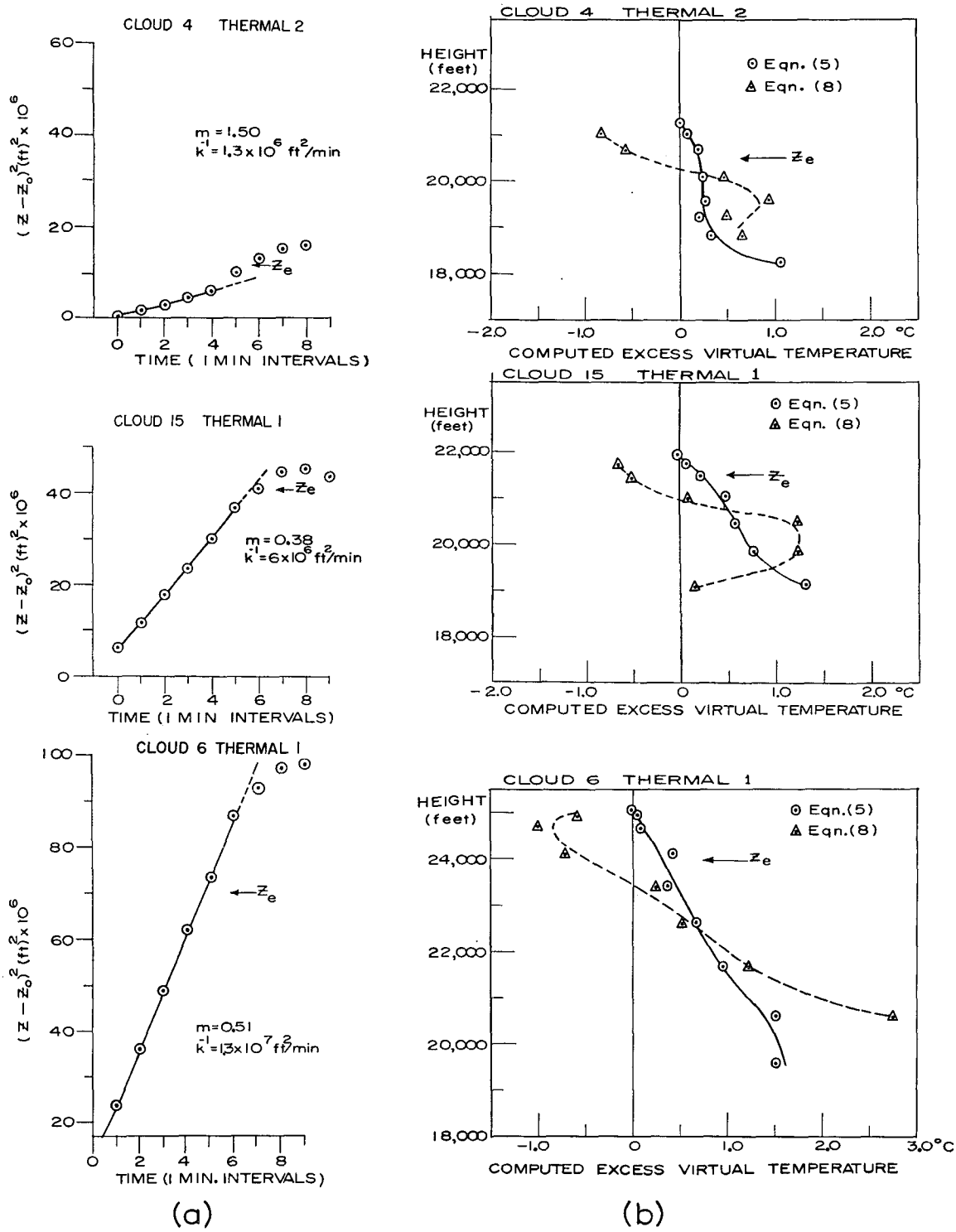

FIG. 12. a) $(Z-Z_0)^2$ versus time (equation 6). Straight line (slope $=k^{-1}$) shows duration where total buoyancy, (equation 5), is conserved. b) Height versus computed excess virtual temperature as determined from equations (5) and (8). Smoothed values of derivatives used in computations.

that small clouds consisted of one or a few easily definable elements (thermals). Thermals associated with small cumulus clouds exhibited a single growth cycle and dissipate without benefit of additional pulsations. Results tended to confirm the view that cumuli consist of comparatively few elements; the larger the cloud dimensions, the larger the element.

Three definite stages in the evolution of a thermal were: the period of uniform expansion with height following saturation, the progressive decrease in diameter (erosion) accompanied by marked vertical declaration, and a subsequent dissipation in all dimensions. In the first stage, broadening was essentially along a cone whose interior angle was about 30°. In this respect, thermals resembled their idealized counterpart in tank and numerical studies. The observed broadening more closely compares with the Scorer-bubble rather than the thermal-capped plume model of Turner which involved a continuing source of buoyant material through the thermal's base. Maximum ascent height appeared to vary with diameter at formation, though it appeared uncorrelated with the initial vertical velocity. The data also indicate some tendency for the total buoyancy to be conserved during broadening.

Application of the results of two mathematical expressions commonly used to describe buoyant bubbles, yield reasonable though somewhat high values of the thermal's mean excess virtual temperature. These computations showed that thermal buoyancy tends to vanish at the erosion level, and become negative above that level.

This study lacked a direct comparison in the deduced buoyancies with actual values. In a future paper, photogrammetric measurements will be supplemented by temperature, liquid water content, vertical velocity, and relative humidity obtained from instrumented aircraft penetrations. It will be possible then to further test the validity of convection models, as well as to relate the additional measurements to the growth cycle observed in cumulus thermals.

Acknowledgments. The authors would like to thank Dr. R. M. Cunningham, of the Cloud Physics Branch, AFCRL, for his criticism and helpful comments. The section on error analysis was done with the assistance of Mr. D. R. Schurz, of the Photogrammetry Laboratory, M. I. T. The study would not have been accomplished without the painstaking photogrammetric measurements carried out by the research personnel of Weather Services, Inc. Computations were made on the AFCRL IBM-650.

REFERENCES

Anderson, C. E., 1960: A study of the pulsating growth of cumulus clouds. *Geophysical Research Papers No. 72,* Air Force Cambridge Research Laboratories, 136 pp.

Braham, R. R., Jr., and M. Draginis, 1960: Roots of orographic cumuli. *J. Meteor.*, **16**, 214–226.

Cunningham, R. M., V. G. Plank and C. M. Campen, 1956: Cloud refractive index studies. *Geophysical Research Papers No. 51,* Air Force Cambridge Research Laboratories, 106 pp.

Hall, W. S., 1960: The rise of an isolated thermal through stratified surroundings. *Aero Rev.*, **34**, 754–755.

Levine, J., 1959: Spherical vortex theory of bubble-like motion in cumulus clouds. *J. Meteor.*, **16**, 653–662.

Lilly, D. K., 1962: On the numerical simulation of buoyant convection. *Tellus*, **14**, pp. 148–172.

Malkus, J. S., 1952: The slopes of cumulus clouds in relation to external wind shear. *Quart. J. R. meteor. Soc.*, **78**, 530–542.

——, 1960: Recent developments in studies of penetrative convection and an application to hurricane cumulonimbus towers. In *Cumulus dynamics.* Proc. of the First Conference on Cumulus Convection, New York, Pergamon Press, 211 pp.

Mason, B. J., and R. Emig, 1961: Ascent of cloudy parcel with mixing. *Quart. J. R. meteor. Soc.*, **87**, 212–222.

Ogura, Y., 1962: Convection of isolated masses of buoyant fluid: a numerical calculation, *J. atmos. Sci.*, **19**, 492–502.

Orville, H. R., and R. A. Kassander, 1961: Terrestrial photogrammetry of clouds. *J. Meteor.*, **18**, 682–687.

Plank, V. G., 1959: Convection and refractive index inhomogeneities. *J. atmos. and terr. Phys.*, **15**, 228–244.

Saunders, P. M., 1961: An observational study of cumulus. *J. Meteor.*, **18**, 451–467.

——, 1962: Penetrative convection into stably stratified fluids. *Tellus*, **14**, 177–194.

Scorer, R. S., 1957: Experiments on convection of isolated masses of buoyant fluid. *J. fluid Mech.*, **2**, 583–594.

——, and F. H. Ludlam, 1953: Bubble theory of penetrative convection. *Quart. J. R. meteor. Soc.*, **79**, 94–103.

Silverman, B. A., 1960: The effect of a mountain on convection. In *Cumulus dynamics.* Proc. of the First Conference on Cumulus Convection, New York, Pergamon Press, 211 pp.

Turner, J. S., 1962: The "starting" plume in neutral surroundings. *J. fluid Mech.*, **9**, 356–368.

Woodward, B., 1959: The motion in and around isolated thermals. *Quart. J. R. meteor. Soc.*, **85**, 144–151.